Exact energy bands and Fermi surfaces of separable Abelian potentials

2001 J. Phys. A: Math. Gen. 34 943

(http://iopscience.iop.org/0305-4470/34/5/302)

INSTITUTE OF PHYSICS PUBLISHING JOURNAL OF PHYSICS A: MATHEMATICAL AND GENERAL

J. Phys. A: Math. Gen. **34** (2001) 943–959 www.iop.org/Journals/ja PII: S0305-4470(01)16442-5

Exact energy bands and Fermi surfaces of separable Abelian potentials

E D Belokolos[1], J C Eilbeck[2], V Z Enolskii[1] and M Salerno[3]

[1] Department of Theoretical Physics, NASU Institute of Magnetism 36-b Vernadsky str., Kiev-680, 03142, Ukraine
[2] Department of Mathematics, Heriot-Watt University, Riccarton, Edinburgh EH14 4AS, UK
[3] Dipartimento di Scienze Fisiche 'E R Caianiello' and INFM Unita' di Salerno, via S Allende, I-84081, Baronissi (SA), Italy

E-mail: bel@imag.kiev.ua, J.C.Eilbeck@hw.ac.uk, vze@imag.kiev.ua and salerno@sa.infn.it

Received 15 August 2000

Abstract

We present a general theory for multidimensional Schrödinger equations with separable Abelian potentials with an arbitrary number of gaps in the spectrum. In particular, we derive general equations which allow one to express the energy and the wavevectors in the Brillouin zone as a function of the spectral parameters. By using the solutions of these equations, we show how to construct the energy bands and the Fermi surfaces in the first Brillouin zone of the reciprocal lattice. As illustrative examples we consider the case of two-dimensional separable potentials with one, two and three gaps in the spectrum. The method can be applied to crystals with a cubic or a rectangular parallelogram Wigner–Seitz cell in arbitrary dimensions. The possibility to generalize the theory to other crystal symmetries is also briefly discussed.

PACS numbers: 7118, 0210, 7120

(Some figures in this article are in colour only in the electronic version; see `www.iop.org`)

1. Introduction

The general theory of the many-dimensional Schrödinger operator was established many years ago, i.e. immediately after the advent of quantum mechanics. Since the pioneering work of Bloch [1], in which the spectral properties of these operators were first recognized to be of fundamental importance for the quantum theory of solids, much work has been done. This lead to the development of the band theory, one of the pillars of modern solid state physics. In spite of this, only a few examples are known of Schrödinger operators with periodic potentials, allowing exact analytical calculations of energy bands and Fermi surfaces.

Although numerical and self-consistent methods to compute the band structure of a solid with good accuracy exist, it is desirable to have exact solutions of the Schrödinger equation. These solutions, for some physically relevant multidimensional periodic potentials, are useful

0305-4470/01/050943+17$30.00

not only for comparison with approximate approaches, but also for further developments of the general theory. This would allow us, for example, to gain a deep understanding of the spectral manifolds and of the corresponding eigenfunctions, as well as of their geometrical and analytical properties.

From a mathematical point of view, the most interesting periodic potentials are those which can be expressed in terms of Abelian functions (Abelian potentials). Abelian functions are multiply periodic functions defined on complex tori, which can be considered in the context of the problem as a suitable complexification of the real crystal lattice and its dual. In some sense they are the analogues of the potentials in classical mechanics which allow a complexification of the Liouville tori leading to Jacobians and Abelian functions and hence to algebraic integrable systems. It is remarkable that although the theory of such potentials was developed long before the advent of quantum mechanics, they have been almost entirely ignored by the solid state physics community. In contrast, we think that these potentials are important and should be considered in solid state physics as being the equivalent of Kepler's problem for atomic physics. They give us the opportunity to study many questions related to the electronic properties of solids in a clear geometrical and analytical form.

In this paper we are interested in multidimensional separable generalizations of the simplest possible Abelian potential, i.e. the one expressed as the Weierstrass elliptic function $\wp(z)$, with one real and one pure imaginary period. The Schrödinger operator with such a potential has exactly one gap spectrum and allows one to obtain eigenfunctions in an explicit form (in the mathematical literature this equation is known as the one-dimensional (1D) Lamé equation). This spectral problem is essentially easier and clearer than, for example, the well known Kronig–Penney problem, and can be used as a building block of a multidimensional theory. Our extensions to this problem are twofold: one is to consider a multi-gap spectrum (a well studied problem), and the second is to extend these multi-gap results to higher dimensions.

The investigation of the 1D Lamé equation was very well developed in the classical monographs of Halphen [2], Krause [3], Forsyth [4] and Whittaker and Watson [5]. Arscott [6, 7] has surveyed results on the Jacobian form of the Lamé equation. The Lamé equation has also figured prominently in a number of recent publications devoted to the study of completely integrable systems of KdV type: Krichever [8], Eilbeck and Enol'skii [9], Enol'skii and Kostov [10], Smirnov [11], Gesztesy and Weikard [12, 13], Zabrodin [14] and others.

The aim of the present paper is to present the general theory for multidimensional Schrödinger equations with separable Abelian potentials with an arbitrary number of gaps in the spectrum (by separable here we mean those potentials which can be written as a sum of N one-dimensional finite-gap potentials, one for each spatial dimension). The introduction of separable Abelian potentials and their application to problems of solid state physics was also considered in [15, 16] for potentials with one and two gaps in the spectrum. Our results allow us to express the energy and the wavevectors in the Brillouin zone (BZ) as a function of the spectral parameters. The edges of the bands also follow from these equations as roots of specific polynomials. From a mathematical point of view this corresponds to the problem of constructing a hyperelliptic N-sheeted covering, $N = g(g+1)/2$ over a torus (elliptic curve), first considered by Jacobi and developed further by Weierstrass, Poincaré and others, see [17, 18] for a detailed exposition.

By using the solutions of these equations for the spectral parameters, we show how one can construct the energy bands and the Fermi surfaces in the first Brillouin zone of the reciprocal lattice. As illustrative examples we consider the case of two-dimensional (2D) separable potentials with a one-, two- and three-gap spectrum. The method, although not restricted to 2D, is apparently applicable only to crystals with a cubic or a rectangular parallelogram

Wigner–Seitz cell. Possible physical applications of our theory, as well as its generalization to other crystal symmetries will be briefly discussed at the end of the paper.

The paper is organized as follow. In section 2 we present the mathematical theory of separable N-dimensional Abelian potentials and the general equations valid in the case of arbitrary gaps in the spectrum. In section 3 we present detailed calculations of bands and Fermi curves for 2D lattices with both square and rectangular symmetry. In the conclusion we discuss possible physical applications of these results to different problems.

2. Separable Abelian g-gap periodic potentials

The N-dimensional Schrödinger operator with the separable potential

$$U(x) = \sum_{k=1}^{N} U_k(x_k) \qquad x = (x_1, \ldots, x_N) \tag{1}$$

has the form

$$\left(-\Delta + \sum_{k=1}^{N} U_k(x_k)\right)\Psi(x) = E\Psi(x) \qquad x = (x_1, \ldots, x_N) \tag{2}$$

and therefore has eigenfunctions of the form

$$\Psi(x_1, \ldots, x_n) = \prod_{k=1}^{N} \psi_k(x_k) \tag{3}$$

where the $\psi_k(x_k)$ satisfy the ordinary differential equations

$$-\frac{\mathrm{d}^2\psi_k(x_k)}{\mathrm{d}x_k^2} + U_k(x_k)\psi_k(x_k) = E_k\psi_k(x_k) \qquad k = 1, \ldots, N. \tag{4}$$

The energy E is of the form

$$E = \sum_{i=1}^{N} E_i = \sum_{i=1}^{N} E(k_i) \tag{5}$$

where $k = (k_i, \ldots, k_N)$ is the wavevector. In the limiting case, when $E(k_i) = k_i^2$ and therefore

$$E = \sum_{i=1}^{N} k_i^2 \tag{6}$$

our approach corresponds to the well known Harrison pseudopotential approach in a theory of electron spectral properties of metals [19]. Hence in this sense our method is a straightforward generalization of the Harrison method.

For simplicity we first discuss the properties of the one-dimensional potentials, the building blocks for the separable N-dimensional potentials in equation (1), by considering the one-gap Lamé potential $U(x) = 2\wp(x)$

$$-\frac{\mathrm{d}^2\Psi(x)}{\mathrm{d}x_k^2} + 2\wp(x)\Psi(x) = E\Psi(x)$$

where $\wp(x)$ is the Weierstrass elliptic function characterized by the curve $w^2 = 4t^3 - g_2t - g_3 \equiv 4(t - e_1)(t - e_2)(t - e_3)$ with parameters g_2 and g_3 given by

$$g_2 = -4(e_1e_2 + e_1e_3 + e_2e_3) \qquad g_3 = 4e_1e_2e_3 \qquad e_1 + e_2 + e_3 = 0 \tag{7}$$

(below we will show how these parameters are related to the boundaries of the spectra). It is known that the eigenfunction and the corresponding eigenvalues of this equation can be expressed as [5]

$$\Psi(x;a) = \frac{\sigma(a-x)}{\sigma(x)\sigma(a)} \exp\{x\zeta(a)\} \qquad E = \wp(a) \tag{8}$$

where a denotes a spectral parameter and σ the Weierstrass σ-function related to the Weierestrass $\wp$ and ζ functions by the relations

$$\zeta(u) = \frac{\partial}{\partial u} \ln \sigma(u) \qquad \wp(u) = -\frac{\partial^2}{\partial u^2} \ln \sigma(u) = -\frac{\partial}{\partial u}\zeta(u).$$

The above wavefunctions can be rewritten in the form of a Bloch function as

$$\Psi(\mathrm{i}x;a) = \mathrm{e}^{\mathrm{i}k(a)x} B(\mathrm{i}x;a) \qquad B(\mathrm{i}x;a) = \frac{\sigma(a-\mathrm{i}x)}{\sigma(\mathrm{i}x)\sigma(a)} \exp\left\{\mathrm{i}\frac{\eta'}{\omega'}ax\right\} \tag{9}$$

where we have taken $x \to \mathrm{i}x$ and introduced the wavevector $k(a)$ as

$$k(a) = \zeta(a) - \frac{\eta'}{\omega'}a. \tag{10}$$

Note that x imaginary does not affect the reality of the potential and it implies that the periodicity of the potential is $\mathrm{Im}(2\omega')$, where $2\omega'$ denotes the imaginary period of the $\wp$ function. The ratio η'/ω' is real since η', the second imaginary period, is purely imaginary. One can then easily prove that (9) is nothing but the Floquet theorem [20] for the one-gap Lamé potential. Indeed, by using the periodicity property of the σ function

$$\sigma(u + 2m\omega + 2m'\omega') = (-1)^{mm'+m+m'}\sigma(u)\,\mathrm{e}^{(u+m\omega+m'\omega')(2\eta m+2\eta' m')} \tag{11}$$

and denoting the translation operator by one period of the potential by $T_{\mathrm{Im}(2\omega')}$, we have that

$$T_{\mathrm{Im}(2\omega')}\Psi(\mathrm{i}x;a) = \Psi(\mathrm{i}x + 2\omega';a) = \mathrm{e}^{\mathrm{i}k(a)\,\mathrm{Im}(2\omega')}\ \Psi(\mathrm{i}x;a) \tag{12}$$

from which we see that Ψ is an eigenfunction of the translation operator associated with the eigenvalue $\mathrm{e}^{\mathrm{i}k(a)\,\mathrm{Im}(2\omega')}$ (this implies that $B(\mathrm{i}x;a)$ is a periodic function with period $\mathrm{Im}(2\omega')$). Note that for the multidimensional separable wavefunction (3), equation (12) automatically leads to the usual Bloch theorem [1]. An equation for the spectral parameter a can be obtained by observing that the function

$$\Lambda(u) = \wp(u) - \wp(a) \tag{13}$$

is a solution of the equation

$$\frac{\mathrm{d}^3\Lambda}{\mathrm{d}^3u} - 4(2\wp(u) + E)\frac{\mathrm{d}\Lambda}{\mathrm{d}u} - 4\wp'(u)\Lambda = 0. \tag{14}$$

Inserting (13) into (14) gives the expression for the energy E in terms of the quantity a

$$E = \wp(a). \tag{15}$$

In this case we simply obtain the relation between the energy and the spectral parameter. However, in the general g-gap case, we will obtain a set of g equations among the spectral parameters. For the $g = 1$ case, equation (15) uniquely determines the energy bands. The reality condition of the energy and the properties of the $\wp$ function imply that the spectrum must lie in the intervals $[e_3, e_2]$ and $[e_1, \infty]$ (see below). Note that equations (10) and (15) express the energy E in terms of the wavevector k in parametric form.

These expressions can be easily generalized to the case of the one-dimensional Schrödinger equation with g-gap Lamé potentials $U(x) = g(g+1)\wp(x)$

$$-\frac{\mathrm{d}^2\Psi(x_k)}{\mathrm{d}x_k^2} + g(g+1)\wp(x_k)\Psi(x_k) = E\ \Psi(x_k).$$

One can check that the eigenfunctions can be written as

$$\Psi(x, a_1, \ldots, a_g) = \mathrm{e}^{\mathrm{i}k(a_1,\ldots,a_g)x} \prod_{j=1}^{g} \frac{\sigma(a_j - \mathrm{i}x)}{\sigma(\mathrm{i}x)\sigma(a_j)} \exp\left\{\mathrm{i}x \sum_{j=1}^{g} \frac{\eta'}{\omega'} a_j\right\} \tag{16}$$

with the wavevector k given by the expression

$$k(a_1, \ldots, a_g) = \sum_{j=1}^{g} \left[\zeta(a_j) - \frac{\eta'}{\omega'} a_j\right]. \tag{17}$$

The equations for the spectral parameters a_j, $j = 1, \ldots, g$ can be determined from the fact that

$$\Lambda(u) = \prod_{j=1}^{g} [\wp(u) - \wp(a_j)] \tag{18}$$

is a solution of the equation

$$\frac{\mathrm{d}^3\Lambda}{\mathrm{d}^3 u} - 4(g(g+1)\wp(u) + E)\frac{\mathrm{d}\Lambda}{\mathrm{d}u} - 2g(g+1)\wp'(u)\Lambda = 0. \tag{19}$$

Inserting (18) into (19) gives the following system of algebraic equations for the quantities $\wp(a_j)$:

$$\alpha_k E S_{k-1} + \beta_k\ g_2 S_{k-2} + \gamma_k g_3 S_{k-3} - \delta_k S_k = 0 \qquad k = 1, 2, \ldots, g \tag{20}$$

where S_k denotes the kth elementary symmetric function

$$S_k = \sum_{j_1 < j_2 < \cdots < j_k}^{g} \wp(a_{j_1})\wp(a_{j_2}) \ldots \wp(a_{j_k}) \tag{21}$$

and

$$\begin{aligned}
\alpha_k &= 4(-1)^{k-1}(k - g - 1) \\
\beta_k &= \tfrac{1}{2}(-1)^{k-1}\left(2(g - (k-4))^3 - 15(g - (k-4))^2 + 37(g - k + 4) - 30\right) \\
\gamma_k &= (-1)^k(g - k + 3)(g - k + 2)(g - k + 1) \\
\delta_k &= 2k(-1)^k\left(4g^2 + 2g(2 - 3k) + 2k^2 - 3k + 1\right).
\end{aligned}$$

(Note that in equation (20) we assume that $S_{-k} = 0$ and $S_0 = 1$.) One can easily check that the first equation (i.e. $k = 1$) of the system in (20) gives the energy E in terms of the quantities a_j, $j = 1, \ldots, g$

$$E = (2g - 1)\sum_{j=1}^{g} \wp(a_j) \tag{22}$$

while the second and third equations ($k = 2, 3$) express the invariants g_2, g_3, in terms of the energy and the quantities a_j, $j = 1, \ldots, g$,

$$g_2 = \frac{8}{g}\left\{\sum_{j=1}^{g} \wp^2(a_j) + \frac{S_2}{g-1}\right\}$$

$$g_3 = \frac{8}{g}\left\{\frac{2g-3}{2g}\sum_{i=1}^{g}\wp^3(a_i) - \frac{1}{g-1}\sum_{i<j}^{g}\left(\wp^2(a_i)\wp(a_j) + \wp(a_i)\wp^2(a_j)\right)\right. \tag{23}$$
$$\left. - \frac{3(2g-3)}{(g-1)(g-2)}S_3\right\}.$$

The other $g-3$ equations establish additional relations between the a_j. To construct the energy bands as a function of k one must solve the above system of algebraic equations for the $\wp(a_j)$ together with a condition for the reality of the energy. In the procedure one must invert the $\wp$ function to obtain the a_j, and use equations to relate the energy E to the wavevectors k in a parametric form. Although this looks complicated it can be easily performed on a computer using one of the many parametric plot packages available.

Before presenting explicit numerical results let us discuss how one can derive from equation (20) the expression for the edges of the bands. We wish to write these bands as a function of the parameters e_1, e_2, e_3 characterizing the underlying elliptic curve. In order to do this one must add to the above general formulae an extra condition which guarantees the reality of the energy (note that since the energy is unknown, we actually have g equations for $g + 1$ unknowns). This can be done by fixing one of the spectral parameters a_i, say a_1, so that $\wp(a_1) = e_i$. One can easily show that this choice will guarantee the reality of the energy. By constructing the Groebner basis for the polynomial in equations (20) one can eliminate the $g - 1$ variables $\wp(a_i)$, $i = 2, \ldots, g$, in favour of the energy. This will lead to factorized polynomials which for $g = 1, 2, 3$, are given, respectively, by

$$4\prod_{i=1}^{3}(E - e_i) \tag{24}$$

$$\left(E^2 - 3g_2\right)\prod_{i=1}^{3}(E + 3e_i) \tag{25}$$

$$E\prod_{i=1}^{3}(E^2 - 6e_iE + 45e_i^2 - 15g_2). \tag{26}$$

It is possible to set up a general procedure to determine these polynomials (and therefore the edges of the bands) for potentials with an arbitrary number of gaps. Thus, for example, for $g = 5, 7, 9$ we obtain

$$(E^2 - 27g_2)\prod_{i=1}^{3}\left[E^3 - 15e_iE^2 + (315e_i^2 - 132g_2)E + 540g_3 + 675e_i^3\right]$$

$$(E^3 - 196g_2E + 2288g_3)\prod_{i=1}^{3}[E^4 - 28e_iE^3 + (1134e_i^2 - 574g_2)E^2$$
$$+ \left(34\,100\,e_i^3 - 5116\,e_ig_2\right)E + 59\,150\,e_i^2g_2 - 528\,983\,e_i^4$$
$$+22\,113\,g_2^2 + 88\,452\,g_3e_i]$$

$$(E^4 - 774g_2E^2 + 21\,600g_3E + 41\,769g_2^2)\prod_{i=1}^{3}[E^5 - 45e_iE^4 + (2970e_i^2 - 1764g_2)E^3$$
$$+(25\,380e_ig_2 - 202\,230e_i^3)E^2 - (9461\,259e_i^4 - 402\,624g_2^2 - 1610\,496g_3e_i$$
$$-1210\,356e_i^2g_2)E - 20\,241\,900e_i^3g_2 + 37\,013\,760e_i^2g_3$$
$$-76\,485\,465e_i^5 + 9253\,440e_ig_2^2].$$

Note that the problem of constructing these polynomials is related to the problem of constructing coverings for hyperelliptic curves on a g-sheeted torus considered by Jacobi, Weierstrass and Poincaré. For Lamé potentials with an arbitrary number of gaps, a solution of this problem can be obtained following techniques described in [5]. Note that the system of equations in (20) refers to the g-gap 1D potential, i.e. to the building blocks of the higher-dimensional cases. In the higher-dimensional separable case one must, of course, consider several such systems, with different spectral parameters and different elliptic curves, one for each dimension. In the case in which the curves coincide, the systems of equations and their corresponding solutions will obviously coincide. These will be discussed in the next section.

3. Energy bands and Fermi curves for 2D separable potentials

From a physical point of view, one is interested in computing the shapes of the energy bands and the corresponding Fermi surfaces as a function of the wavenumbers in the first BZ. From this knowledge, important physical properties of the system will follow, such as the density of states, the electron effective mass, transport properties, etc. In this section we will show how this can be done exactly for 2D separable elliptic potentials with one, two and three gaps in the spectrum, using the theory described above (for simplicity we restrict ourselves to the 2D case, but the construction is quite general and can be applied to 3D as well). This will cover the cases of crystals with a square or rectangular Wigner–Seitz cell and with two, three or four energy bands, respectively.

More specifically, let us consider the potential

$$U(x, y) = g(g+1)(\wp(\mathrm{i}x + \omega) + \wp(\mathrm{i}y + \tilde{\omega})) \tag{27}$$

associated with two elliptic curves $w^2 = 4t^3 - g_2t - g_3$ and $\tilde{w}^2 = 4t^3 - \tilde{g}_2t - \tilde{g}_3$ (one for each spatial direction) with g_2, g_3 (and similarly for $\tilde{g}_2$, $\tilde{g}_3$ and $\tilde{e}_i$, $i = 1, 2, 3$) related to the gap edges $e_i, i = 1, 2, 3$ by equations (7). Note that in order to have a real and non-singular potential for all $x, y \in R$, we have taken the argument of the $\wp$ functions appearing in the potential, along the imaginary axis shifted by the half-real periods $\omega, \tilde{\omega}$ of the corresponding elliptic curve (recall that the $\wp$ function is singular at the origin). This implies that the periodicity in the x and y directions are just the two imaginary periods $2\omega'$, $2\tilde{\omega}'$.

We shall first consider the case of identical elliptic curves, this corresponding to lattices with square Wigner–Seitz cells (the periodicity of the potential in the x and y directions being the same). The case of different curves, associated with rectangular Wigner–Seitz cells, will be discussed at the end of this section. In the following calculation we fix the parameters $e_1 = 2$, $e_2 = -0.5$, $e_3 = -1.5$ (and $\tilde{e}_i = e_i$), this corresponds to having fixed the real and the imaginary periods

$$\omega = \int_{e_3}^{e_2} \frac{\mathrm{d}t}{\sqrt{4t^3 - g_2t - g_3}} \qquad \omega' = \int_{e_2}^{e_1} \frac{\mathrm{d}t}{\sqrt{4t^3 - g_2t - g_3}}$$
$$\eta = \int_{e_3}^{e_2} \frac{t\,\mathrm{d}t}{\sqrt{4t^3 - g_2t - g_3}} \qquad \eta' = \int_{e_2}^{e_1} \frac{t\,\mathrm{d}t}{\sqrt{4t^3 - g_2t - g_3}}$$

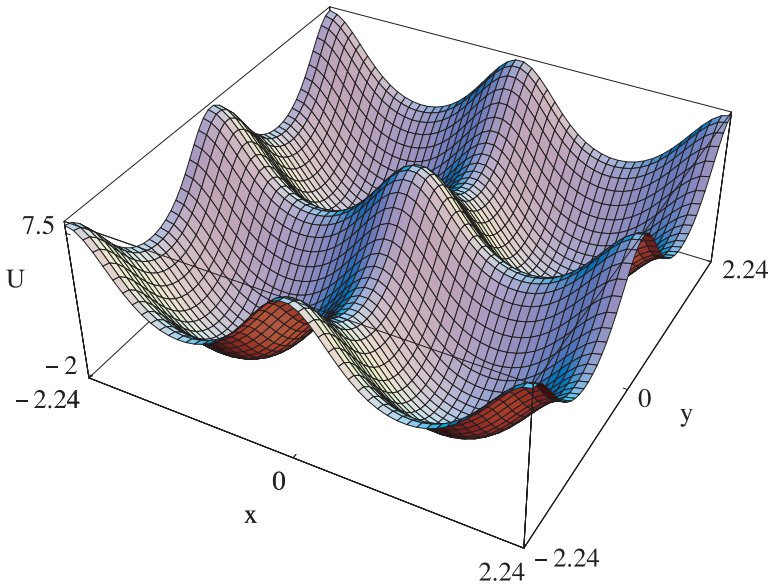

Figure 1. Potential profile in the one-gap case with parameters values $e_1 = 2, e_2 = -0.5, e_3 = -1.5$.

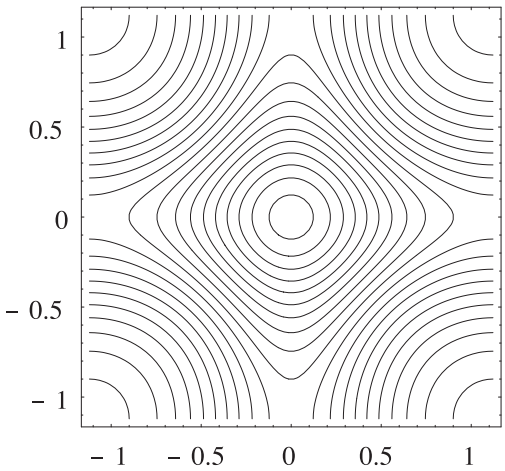

Figure 2. Level curves of the potential in figure 1.

as $2\omega = 1.823\,39$, $2\omega' = 2.241\,76\,\mathrm{i}$, $2\eta = 1.7851$, $2\eta' = -1.251\,19\,\mathrm{i}$ (note that Legendre's relation [5]: $\eta\omega' - \eta'\omega = \mathrm{i}\frac{\pi}{2}$ is satisfied).

In real applications, since the e_i's determine the edges of the energy bands, one should consider them as parameters to be fixed by experiment. Let us start with the one-gap potential ($g = 1$ in equation (27)) which, being simple, will be used to fix the notation and to check the results. This potential is plotted in figure 1 as a function of x, y, from which we see that it is periodic (with the same period in both directions given by $2|\omega'|$), real and well behaved over all space. In figure 2 the level curves of such potentials are reported in the Wigner–Seitz cell. From equations (20) we have for this case only one equation ($g = k = 1$) which expresses the

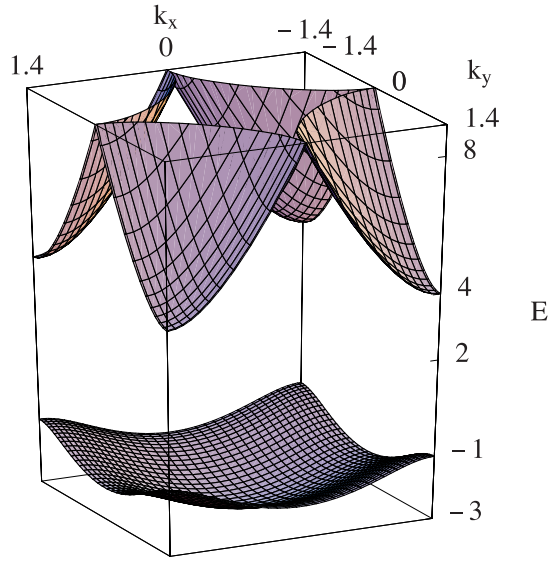

Figure 3. Energy bands of the first Brillouin zone for the potential in figure 1. The edges of the Brillouin zone (i.e. $\pm\frac{\pi}{2|\omega'|}$) for the parameters chosen in figure 1 correspond to the values $\pm 1.401\,396$.

energy as a function of the 'spectral' parameters: $E = \wp(a_1) + \wp(\tilde{a}_1)$. Since the energy is additive in the $\wp(a_i)$, the spectral parameters must vary on curves of the fundamental domain on which $\wp$ is real. These curves coincide with the intervals $[0, 2\omega]$ and $[\omega', 2\omega + \omega']$ in correspondence to which the wavevectors $k_x = \zeta(a_1) - \frac{\eta'}{\omega'}a_1$, $k_y = \zeta(\tilde{a}_1) - \frac{\eta'}{\omega'}\tilde{a}_1$ will span the BZ $\left[-\frac{\pi}{2|\omega'|}, \frac{\pi}{2|\omega'|}\right] \times \left[-\frac{\pi}{2|\omega'|}, \frac{\pi}{2|\omega'|}\right]$.

The energy bands in k-space are then obtained by plotting E, k_x, k_y parametrically as functions of $a_1, \tilde{a}_1$ in the above intervals. This is shown in figure 3, from which we see that the ranges of the lower and upper bands are $[-3, -1]$ and $[4, \infty]$, respectively. In terms of the spectral parameters this corresponds to taking $a_1, \tilde{a}_1 \in [\omega', 2\omega + \omega']$, for the lower band, and $a_1, \tilde{a}_1 \in [0, 2\omega]$ for the upper one. This is evident from the fact that $\wp(\omega') = e_3 = -1.5$, $\wp(\omega + \omega') = e_2 = -0.5$ and $\wp(\omega) = e_1 = 2$ (the band edges are simply twice these values). Also note that for bands symmetric in k (as in our case) one can restrict to only half of these parameter intervals (the other half just reproduces the symmetry). Since for a given band the energy is a continuous function of k_x, k_y, one can draw curves of constant energy which are analogous to the equipotential surfaces of electrostatics. One of these curves will be the so-called Fermi curve, i.e. the curve for which all states described by k-vectors within it will be occupied and all k-vectors outside it will label unoccupied states. One can easily show that this curve (in the 3D case a surface) has the symmetry of the crystal, i.e. it is invariant under the point group operations characterizing the lattice.

In figure 4 we plot the Fermi curves, i.e. the curves of constant energy, as a function of k_x, k_y for different values of E. Note that at the bottom and at the top of the bands, the Fermi curve are circles, as for the free-electron case, whilst for intermediate values they deform and intersect the BZ boundaries perpendicularly. This fact is an indirect check on the correctness of our calculations since from the general theory it is known that the Fermi curve is always tangential to $\nabla E(k)$ and, for any reciprocal lattice vector K perpendicularly joining opposite parallel faces of the BZ, one must have that $K \cdot \nabla E(k) = 0$. In figure 5 the Bloch wavefunction

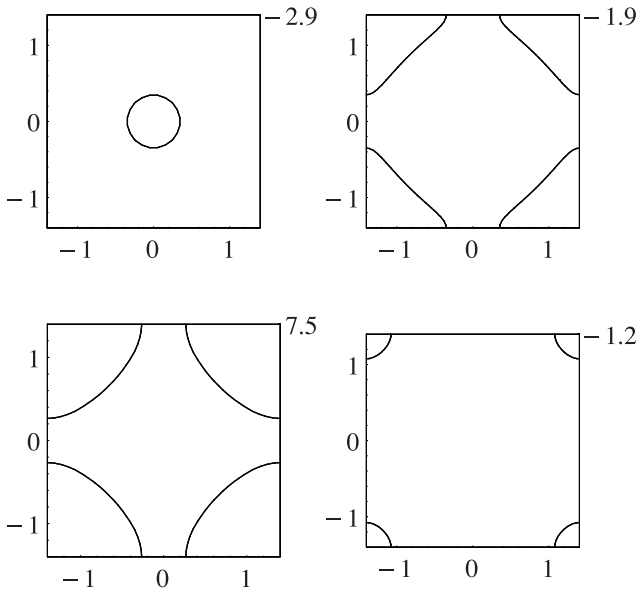

Figure 4. Fermi curves relative to the energy bands of figure 3. The constant energy value at which the curves are taken is reported at the top right-hand side of each figure

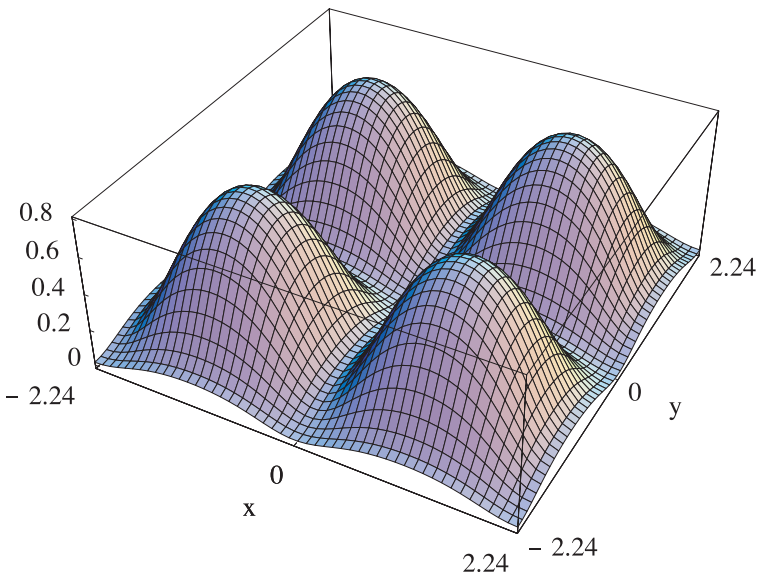

Figure 5. Modulo squared wavefunction of the ground state for the potential in figure 1. The energy is $E = -3$, corresponding to the bottom of the first band in figure 2.

at the bottom of the lower band (ground state) is shown. It is an extended function both in x and y and has maxima located corresponding to the potential minima.

Let us now consider the case of two gaps in the spectrum ($g = 2$ in equation (27)). From the system (20) we have two equations, one for the energy and another for g_2 as a function of the spectral parameters a_1, a_2. These equations can be easily solved by taking a_1 (similarly

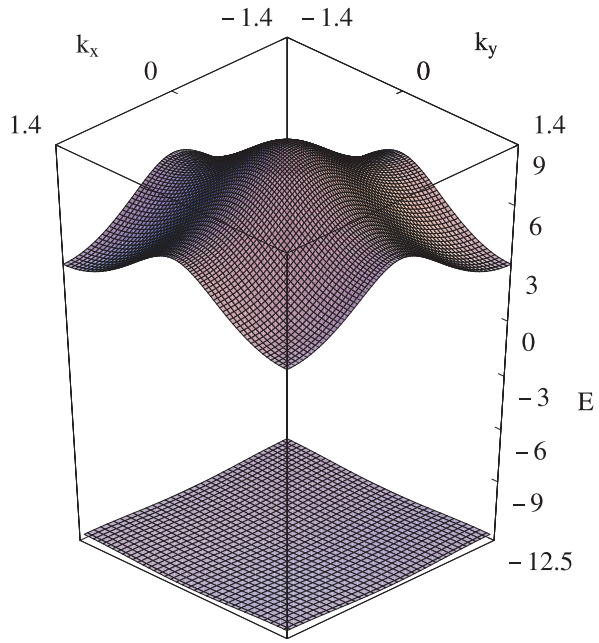

Figure 6. The lowest two energy bands for a separable two-gap potential characterized by the parameters given in figure 1.

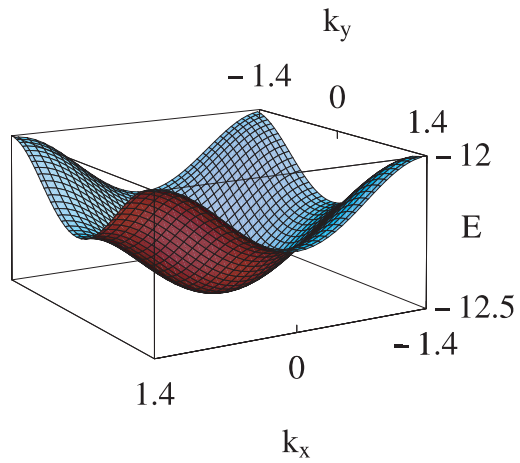

Figure 7. The lower band in figure 6 reported on a larger scale.

for $\tilde{a}_1$) varying over the same intervals as for the $g = 1$ case (this is a requirement for the reality of the energy), and then solving the resulting quadratic equation for $\wp(a_2)$ involving g_2. By inverting the Weierstrass $\wp$ function we obtain a_1, a_2, which can then be used to plot the energy as a function of the wavenumbers. In figure 6 the two lower bands for the 2D two-gap potential are plotted for the same parameters as before. In figure 7 we have shown the lowest band in greater detail (the highest energy band is similar to that of $g = 1$ and was omitted for graphical convenience). In figures 8 and 9, a set of Fermi curves for the two lowest bands are also shown. From these figures we see that the Fermi curves have the same qualitative

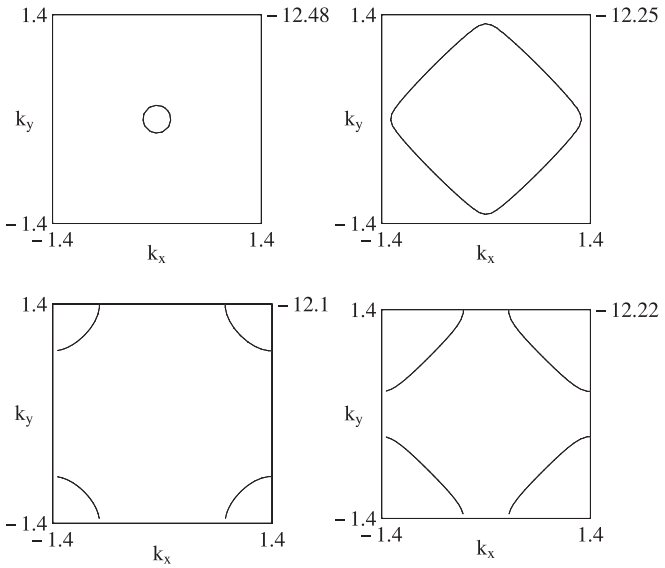

Figure 8. Fermi curves relative to the first (lower) band of figure 6. The top right-hand side of each figure shows the constant energy value at which the curve is taken.

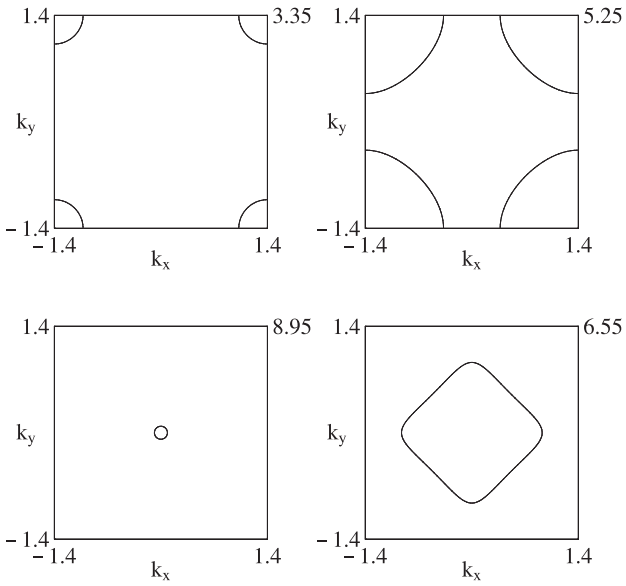

Figure 9. Same as in figure 8 but for the second band of figure 6.

behaviour as for the $g = 1$ case, with a fourfold symmetry with respect to the centre of the Brioullin zone. In figure 10 the energy is plotted as a function of the spectral parameter along the lines $a_i = \tilde{a}_i$, from which we see that the edges of the bands are in agreement with the formula in equation (25) (in our case $g_2 = 13$).

A similar analysis can be done for the three-gap case. Now besides the energy and the equation for g_2 we also have the equation for g_3. To find the spectral parameters a_1, a_2, a_3 in

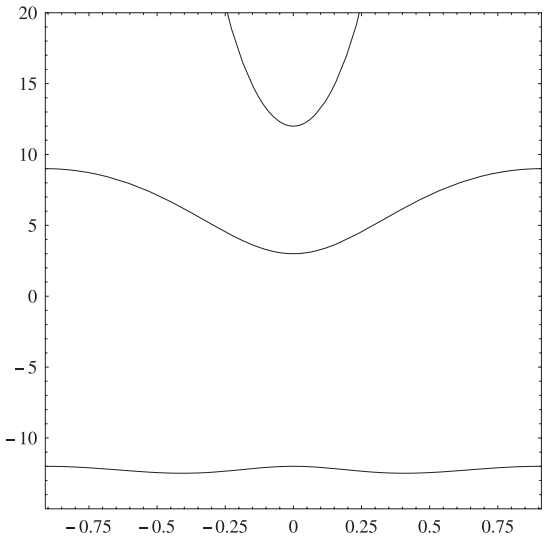

Figure 10. Energy curves as functions of the spectral parameters for $\alpha = \beta \in [-\omega/2, \omega'/2]$. The edges of the energy bands are $-2\sqrt{3g_2},\ -6e_1,\ -6e_2,\ -6e_3,\ 2\sqrt{3g_2}$, with e_1, e_2, e_3 as in figure 1.

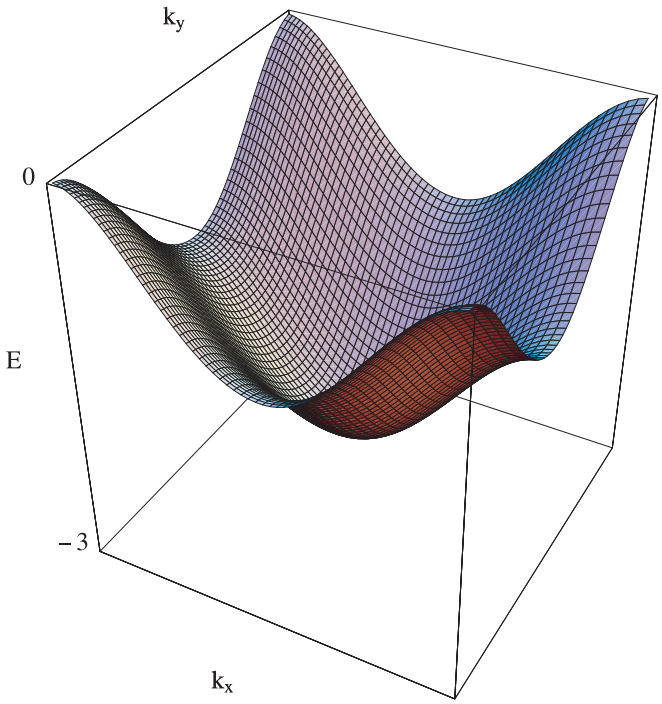

Figure 11. The second lowest energy band for the three-gap case. The parameters of the curves are fixed as in figure 1.

this case, one must solve a quadratic and a sextic equation numerically. Since the energy bands look qualitatively similar to those depicted in the previous cases, in figure 11 we show only the second lowest band and in figure 12 the corresponding Fermi curves. Note that the small

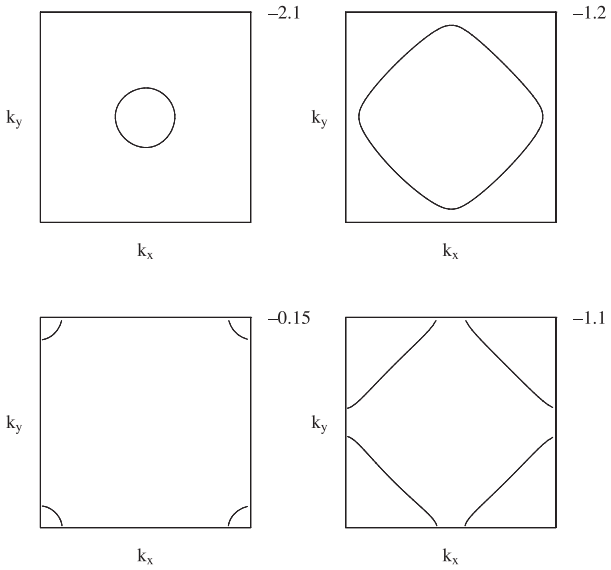

Figure 12. Fermi curves relative to the band in figure 11.

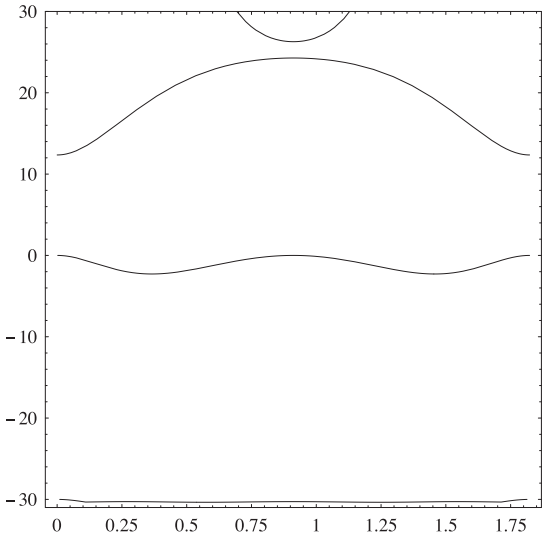

Figure 13. Energy curves as functions of the spectral parameters for $\alpha = \beta \in [0, 2\omega]$ for the three-gap case. The edges of the energy bands are the root of the polynomial in equation (26).

gaps between the Fermi curves and the boundaries of the Brillouin zone are due to numerical effects (we stopped before intersecting the boundary since one needs higher precision i.e. longer computer time, to calculate the solution in these regions). It is evident, however, that the intersection of the Fermi curve with the edges of the Brillouin zone are always orthogonal. In figure 13 the energy bands are shown as functions of the spectral parameters. It is interesting to note that the shape of the bands are different from those in the reciprocal space (the second lowest band, for example, has a maximum in the centre as a function of the spectral parameter,

while it has a minimum as a function of the wavenumbers). The edges of these bands are

$$E = 0 \qquad E = 3e_i \pm \sqrt{9e_j^2 + 15(e_j - e_k)^2} \tag{28}$$

plus cyclic permutations of $i, j, k = 1, 2, 3$, which are just the roots of the polynomial in equation (26) (these values agree with the energy gaps derived by Smirnov in his reduction studies of elliptic potentials [21]).

Before closing this section we wish to discuss the case of lattices with rectangular Wigner–Seitz cells. This corresponds to the general case of different elliptic curves associated with each space direction. In figure 14 the level sets of a potential of this type are plotted (small circles correspond to maxima and large ones to minima). Here the periodicity in the x direction is characterized by the same elliptic curve as before, but for that in the y direction we take the curve with parameters $\tilde{e}_1 = 4$, $\tilde{e}_2 = -1$, $\tilde{e}_3 = -3$ and with real and imaginary periods given by $2\tilde{\omega} = 1.823\,39$, $2\tilde{\omega}' = 2.241\,76\,\mathrm{i}$, $2\tilde{\eta} = 1.7851$, $2\tilde{\eta}' = -1.251\,19\,\mathrm{i}$. The Brillouin zone is then also rectangular with extensions $\left[-\frac{\pi}{2|\omega'|}, \frac{\pi}{2|\omega'|}\right] \times \left[-\frac{\pi}{2|\tilde{\omega}'|}, \frac{\pi}{2|\tilde{\omega}'|}\right]$. In figure 15 the two bands of the $g = 1$ potential on a rectangular lattice are reported as a function of wavevectors in the first BZ. In contrast with the square lattice case, both bands are asymmetric in the two directions, with edges given by $-4.5, -1.5, 6$. These numbers are just the sums of the edges of the two separate elliptic curves, $e_1 + \tilde{e}_1$, $e_2 + \tilde{e}_2$, $e_3 + \tilde{e}_3$. Moreover, from figure 16 we see that, due to the asymmetry, the Fermi curves intersect the Brioullin zone boundaries first in k_y and then in the k_x direction.

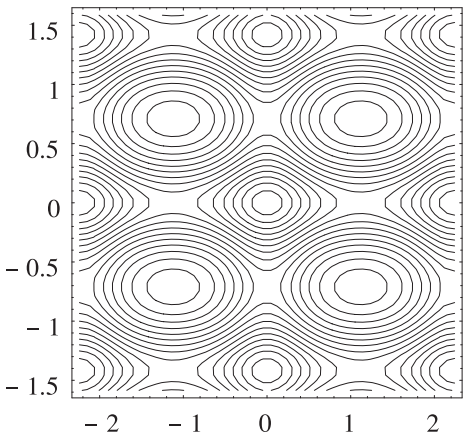

Figure 14. Level curves of the one-gap potential characterized by two different curves. The first curve characterizing the x direction has the same parameters as in figure 1, whilst the other has the parameter $\tilde{e}_1 = 4, \tilde{e}_2 = -1, \tilde{e}_3 = -3$.

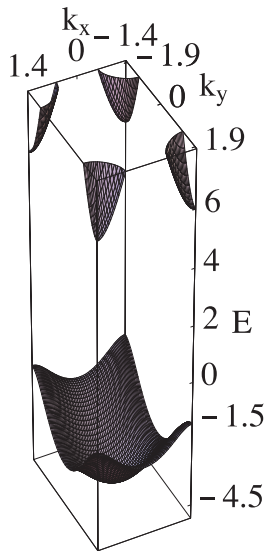

Figure 15. Energy bands in the first Brillouin zone for the potential in figure 14.

It is interesting to note that, although the Fermi curve approaches the boundary tangentially, after the intersection it always becomes orthogonal to it. We also note that at the bottom and at the top the behaviour is very similar to that for square lattices, i.e. the curves are circles as for free electrons. From this analysis one can easily obtain a qualitative picture of the behaviour of the bands and of the Fermi curves for the multigap 2D potentials on rectangular lattices,

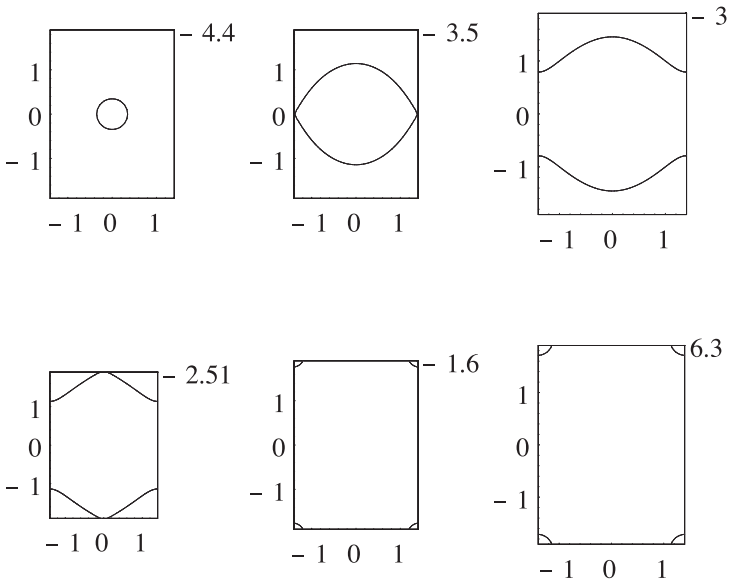

Figure 16. Fermi curves in the first Brillouin zone for the bands in figure 15.

and therefore we will not discuss them further here. In closing this paper we wish to note that with semiconductor nano-technologies, it is possible today to construct artificial solids in 2D as arrays of quantum dots [22]. With electrode deposition techniques [23], it could indeed be possible to construct periodic gates on top of a quantum well so as to create smooth 2D potentials of the type described in this paper. Moreover, the generalization of our analysis to 3D potentials, with a Wigner–Seitz cell which is a cube or a rectangular parallelogram, can easily be done.

We hope to generalize our results to lattices of some other spatial symmetry by means of the Trebich–Verdier and Smirnov potentials (see, e.g., [24]). However, the extension of this method to lattices of general spatial symmetry with separable multidimensional Lamé potentials seems problematic. In this case, however, potentials arising from hyperelliptic extensions of this theory, can be useful. This generalization is presently under investigation [25].

Acknowledgments

The research of the second and fourth authors was supported in part by the INTAS grant 93-1324-Ext. The research of the third author was supported in part by the CRDF grant and INTAS grants 93-1324-Ext and INTAS-96-770. JCE and MS are also grateful for support under the LOCNET EU network HPRN-CT-1999-00163.

References

[1] Bloch F 1928 Quantum mechanics of electrons in crystal lattices *Z. Phys.* **52** 555–600
[2] Halphen G H 1888 *Traité des Fonction Elliptiques* vol 2 (Paris: Gauthier-Villars)
[3] Krause M 1895 *Theorie der doppeltperiodischen Funktionen einer veränderlichen Grösse* vol 1 (Leipzig: Teubner)
[4] Forsyth A R 1959 *Theory of Differential Equations* (New York: Dover) part I, II, vol 4

[5] Whittaker E T and Watson G N 1969 *A Course of Modern Analysis* (Cambridge: Cambridge University Press)
[6] Arscott F M and Khabaza I M 1962 *Tables of Lamé Polynomials (Mathematical Tables Series vol 17)* (Oxford: Pergamon)
[7] Arscott F M 1964 *Periodic Differential Equations: an Introduction to Mathieu, Lamé and Allied Functions (International Series of Monographs in Pure and Applied Mathematics vol 66)* (Oxford: Pergamon)
[8] Krichever I M 1980 Elliptic solutions of the Kadomtsev–Petviashvili equation and integrable systems of particles on a line *Funct. Anal. Appl.* **14** 282–90
[9] Eilbeck J C and Enol'skii V Z 1994 Elliptic Bake–Akhiezer functions and an application to an integrable dynamical system *J. Math. Phys.* **35** 1192–201
[10] Enol'skii V Z and Kostov N A 1994 On the geometry of elliptic solitons *Acta Appl. Math.* **36** 57–8
[11] Smirnov A O 1994 Finite-gap elliptic solutions of the KdV equation *Acta Appl. Math.* **36** 125–66
[12] Gesztesy F and Weikard R 1995 Lamé potentials and the (m)KdV hierarchy *Math. Nachr.* **176** 73–91
[13] Gesztesy F and Weikard R 1998 Elliptic algebro-geometric solutions of the KdV and AKNS hierarchies—an analytic approach *Bull. AMS* **35** 271–317
[14] Zabrodin A 1999 On the spectral curve of the difference Lamé operator *IMRN* **11** 589–614
[15] Bar'yakhtar V G, Belokolos E D and Korostil A M 1992 A new method for calculating the electron spectrum in solids: application to high-temperature superconductors *Phys. Status Solidi* (b) **169** 105–14
[16] Bar'yakhtar V G, Belokolos E D and Korostil A M 1993 Method of separable finite-band potential: a new method for calculating electron energy spectrum of solids *Phys. Metals* **12** 829–38
[17] Krazer A 1903 *Lehrbuch der Thetafunctionen* (Leipzig: Teubner) (1998 reprinted by Chelsea)
[18] Belokolos E D, Bobenko A I, Enol'skii V Z, Its A R and Matveev V B 1994 *Algebro Geometrical Aproach to Nonlinear Integrable Equations* (Berlin: Springer)
[19] Harrison W A 1966 *Pseudopotentials in the Theory of Metals* (New York: Benjamin)
[20] Floquet G 1883 Sur les equations différentielles linéaires á coefficients périodiques *Ann. Sci. École Norm., Super.* **XII** 47–89
[21] Smirnov A O 1997 On a class of elliptic potentials of the Dirac operator *Math USSR Sbornik* **188** 115–35
[22] Jacak L, Hawrylak P and Wojs A 1998 *Quantum Dots* (Berlin: Springer)
[23] Kotthaus J P, Alsmeier J and Batke E 1990 Voltage-tunable quantum dots on silicon *Phys. Rev.* B **41** 1699–702
[24] Bar'yakhtar V G, Belokolos E D and Korostil A M 1993 Fermi-surfaces of metals with *fcc* structures in the model of finite-band potential *Metalofizika* **15** 3–13 (in Russian)
[25] Buchstaber V M, Eilbeck J C, Enol'skii V Z, Leykin D V and Salerno M 2000 Multidimensional Schrödinger equations with Abelian potentials, submitted